Journal Name

ARTICLE TYPE

Cite this: DOI: 00.0000/xxxxxxxxxx

Topological defects of integer charge in cell monolayers†

Kirsten D. Endresen,[a] MinSu Kim,[a] Matthew Pittman,[b] Yun Chen,[b] and Francesca Serra *[a]

Supplemental Materials

Video captions

Video V1: Phase contrast image of fibroblasts 3T6 growing on a pattern with 100μm spacing between ridges. Inside the inner circle with +1 topological charge, initially the cells are isotropic. As density increases, cells start to aling along one direction and two defects with charge +1/2 are formed close to the inner ridge.

Video V2: Phase contrast image of fibroblasts 3T6 growing on a pattern with 100μm spacing between ridges. Two defects with charge +1/2 are formed between the first and the second ridge.

[a] *Johns Hopkins University, Dept. Physics and Astronomy, Baltimore, USA, E-mail: francesca.serra@jhu.edu*
[b] *Johns Hopkins University, Dept. Mechanical Engineering, Baltimore, USA*
† Electronic Supplementary Information (ESI) available: [details of any supplementary information available should be included here]. See DOI: 00.0000/00000000.

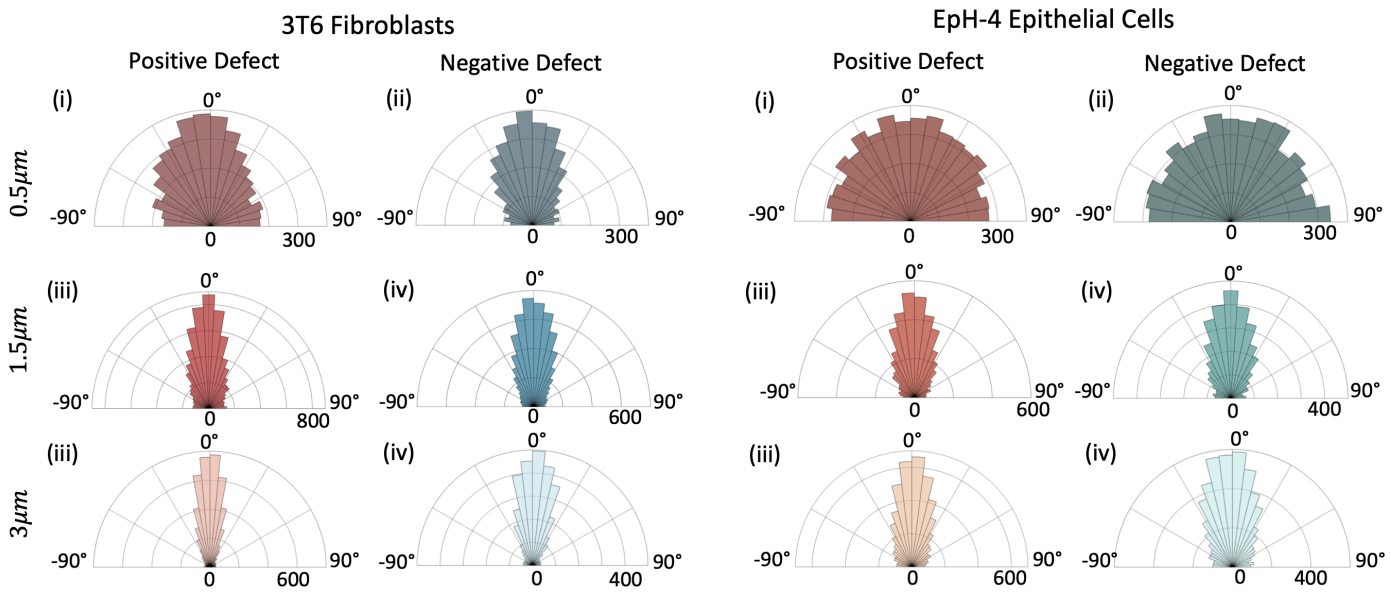

Fig. 1 Cell alignment on ridges with varying height. On the left, 3T6 fibroblast alignment near defects with charge +1 and -1 for r=60μm patterns with ridge height 0.5, 1.5 and 3μm. On the right, EpH-4 epithelial cells alignment near defects with charge +1 and -1 for r=30μm patterns with ridge height 0.5, 1.5 and 3μm. (a) (i) n=5 samples, $\sqrt{\langle\alpha^2\rangle}$=46°. (ii) n=4, $\sqrt{\langle\alpha^2\rangle}$=39°. (iii) n=5, $\sqrt{\langle\alpha^2\rangle}$=37°. (iv) n=5, $\sqrt{\langle\alpha^2\rangle}$=34°. (v) n=5, $\sqrt{\langle\alpha^2\rangle}$=28°. (vi) n=4, $\sqrt{\langle\alpha^2\rangle}$=30°. (b) (i) n=5, $\sqrt{\langle\alpha^2\rangle}$=50°. (ii) n=5, $\sqrt{\langle\alpha^2\rangle}$=51°. (iii) n=4, $\sqrt{\langle\alpha^2\rangle}$=35°. (iv) n=3, $\sqrt{\langle\alpha^2\rangle}$=36°. (v) n=5, $\sqrt{\langle\alpha^2\rangle}$=37°. (vi) n=5, $\sqrt{\langle\alpha^2\rangle}$=37°.

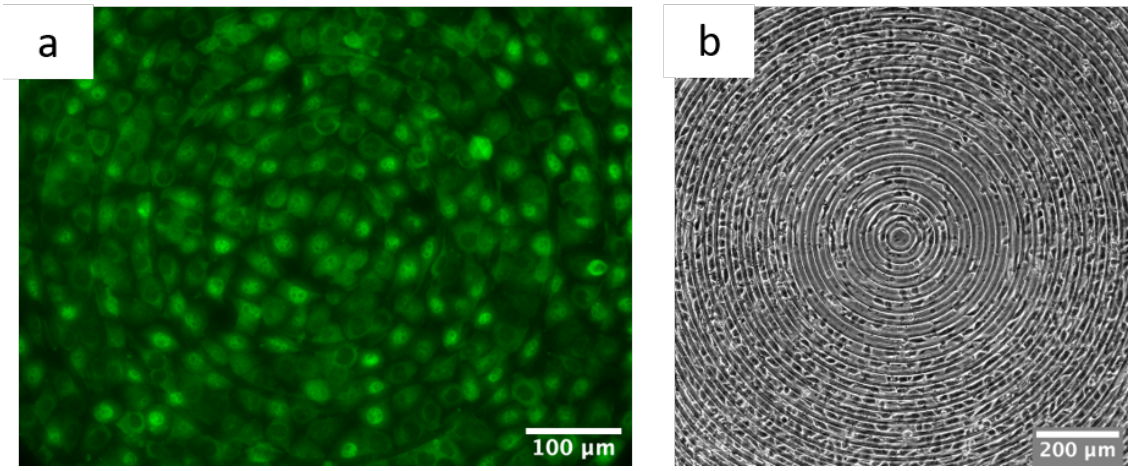

Fig. 2 Epithelial cell monolayers on patterns with tall ridges. (a) The fluorencence indicates the expression of YAP, explained in detail in Section 2.3. The ridges are 2.1μm tall. It is possible to detect by eye the location of the ridges as cells do not grow easily on them, indicating that the tall ridges can disrupt the continuity of the monolayer - for this reason, we avoid them. This image is then reprised in the paper as Fig. 5d. (b) Epithelial cells on 3μm-tall ridges. The cells expand not uniformly. In particular, they are often prevented from filling the inner layers near the defects. We do not detect these effects using 1.5-μm ridges.

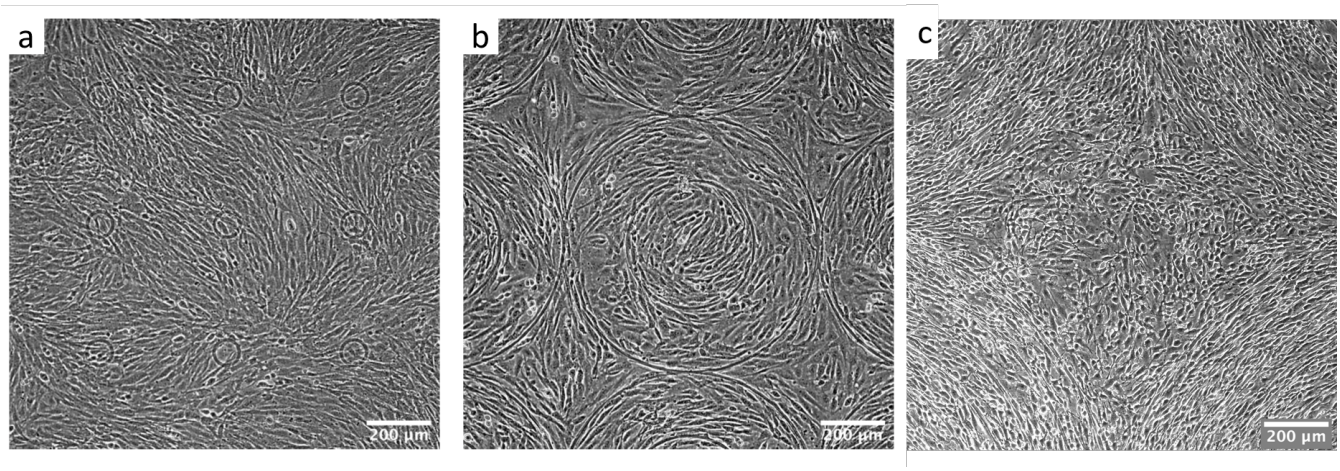

Fig. 3 Fibroblasts growing on small circular 1.5μm tall ridges. (a) Fibroblasts can be seeing going over the ridges and ordering randomly throughout. (b) Fibroblasts growing on patterns with only two ridges. Here, as the length-scale of the separation between ridges is around 100μm, they can align and form defects as imposed by the pattern. (c) If the separation between ridges is too wide, cells will form many more defects in the region between ridges, as shown in this example where only +1 defects are patterned and -1 are not.

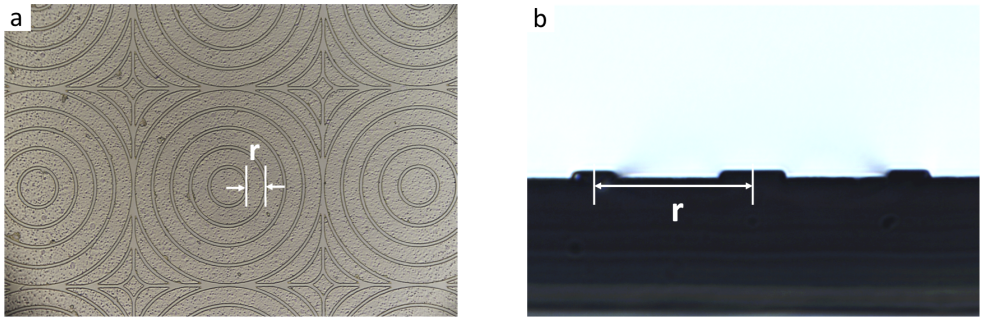

Fig. 4 (a) Top view of patterned PDMS, where r is the spacing between ridges. (b) Cross section of the ridges of the PDMS pattern.

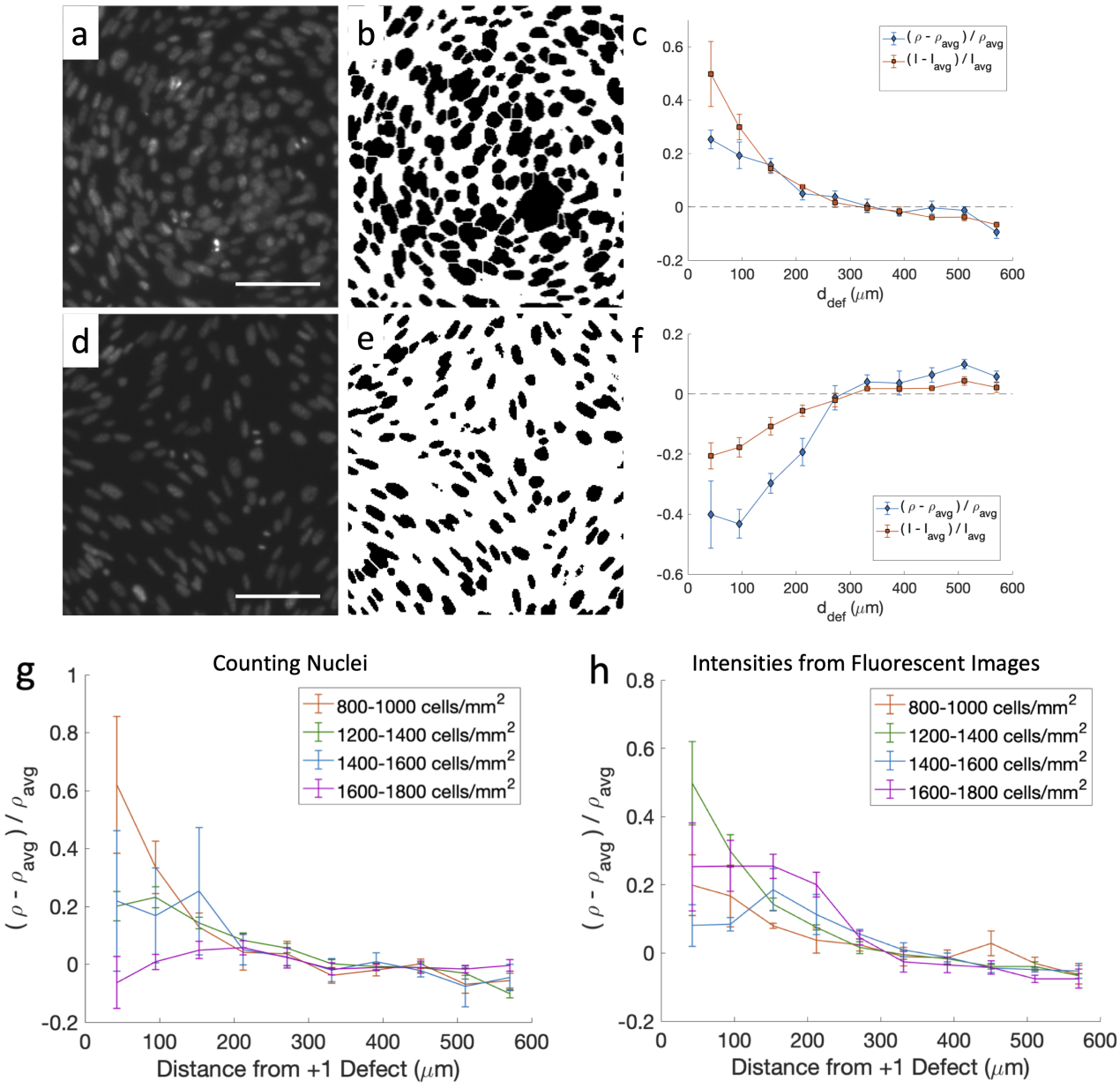

Fig. 5 (a) Fluorescent image of 3T6 nuclei near the center of the +1 defect when cells had ρ_{avg}=1325 cells/mm^2. (b) Binary mask comparison used to fit ellipses. At this density, cells at the center of the +1 defect become too close together to accurately separate using our ImageJ analysis method, leading to an underestimate of the density in the center of the +1 defect. (c) Decay of the density away from the defect computed from the ellipse fitting method described in Methods compared with the change in the image intensity away from the defect, normalized by the average image intensity. Both methods in this case capture the increased density in the vicinity of a +1 defect. n=5 samples. (d) Fluorescent image of 3T6 nuclei near the center of a -1 defect when cells had ρ_{avg} 1277 cells/mm^2. Scale bars are 100μm. (e) Binary mask comparison. Since the cells are more sparse near the -1 defect, the analysis method of fitting ellipses to the nuclei remains feasible at higher average densities. (f) Change in density away from the -1 defect compared to the change in image intensity. n=5 samples. At low density, cell counting provides a more accurate method to measure cell density, while the differences are less marked at low fluorescence intensity between the negative defect and the rest of the sample. (g) Cell density variation calculated with cell counting. Due to the under-counting of cells in the nucleus, the image shows that the accumulation near +1 defects is not captured by the ellipse fitting method of analysis for $\rho_{avg} > 1600$ cells/mm^2. However, the image intensity method of analysis (h) captures the observed density increase, even at high densities. Statistics: (g) For ρ_{avg}=800-1000 cells/mm^2, n=7 samples. For ρ_{avg}=1200-1400 cells/mm^2, n=11. For ρ_{avg}=1400-1600 cells/mm^2, n=11. For ρ_{avg}=1600-1800 cells/mm^2, n=8. (h) n=5 for every density.

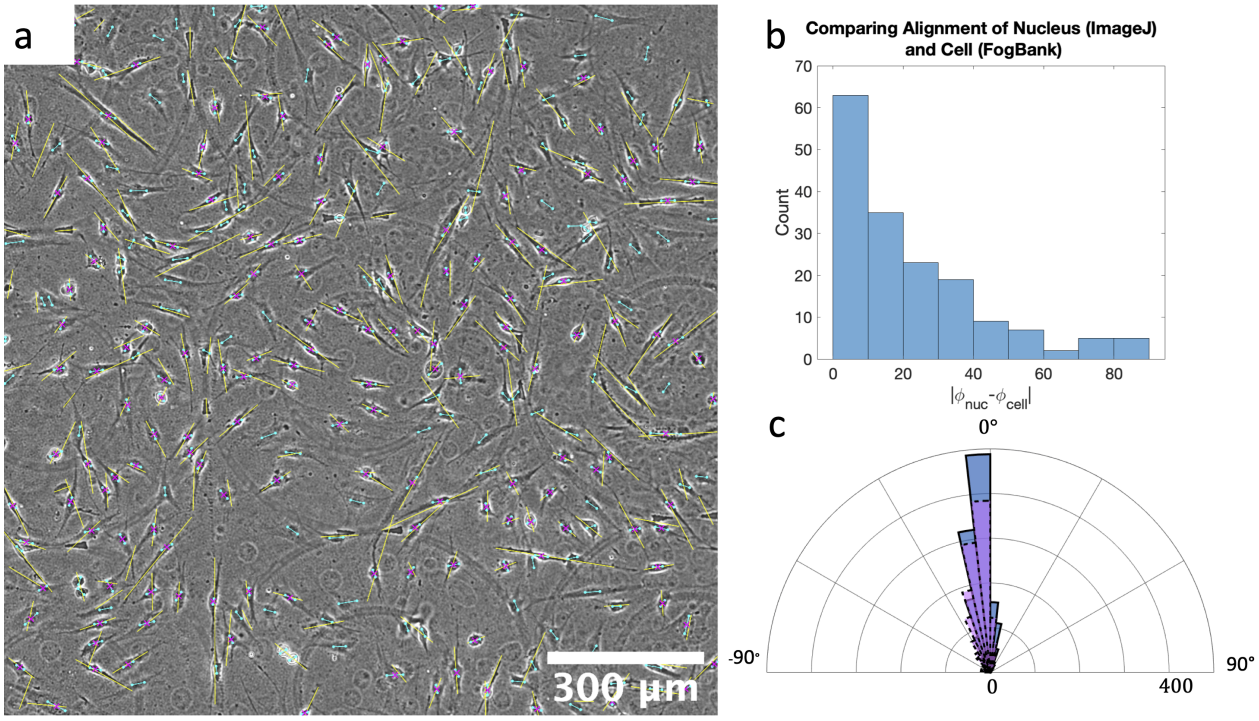

Fig. 6 Comparison between cell orientation estimated with nuclear staining and with cell image analysis. (a) Image of cell orientation analyzed at low density with FogBank (yellow glyphs) and orientation obtained by nuclei (blue arrows). Magenta crosses indicate cells which were identified by both methods (n=168). (b) Graph estimating the distribution of discrepancies in the angle measurements with the two methods for the 168 identified pairs, where ϕ_{nuc} and ϕ_{cell} represent the major axis angle identified from the fluorescent image and the phase contrast image (using FogBank), respectively. (c) Alignment obtained for a confluent sample of 3T6 cells (ρ_{avg}=1399 cells/mm^2) on r=60μm patterns with the two methods. The nuclear staining method underestimates the degree of alignment compared to the segmentation method, but the distribution are consistent.

.